THE ASTROPHYSICAL JOURNAL, 311:864–872, 1986 December 15

A LINEAR SURVEY OF THE MIRA VARIABLE STAR INSTABILITY REGION OF THE HERTZSPRUNG-RUSSELL DIAGRAM

DALE A. OSTLIE
Physics Department, Weber State College, Ogden, Utah
AND
ARTHUR N. COX
Theoretical Division, Los Alamos National Laboratory, University of California
Received 1986 January 16; accepted 1986 May 20

ABSTRACT

An extensive linear pulsation study of Mira variable stars has been carried out. Approximately 100 models were calcuated for 0.8, 1.0, 1.4, and 2.0 $M_\odot$ stars with effective temperatures from 2700 K to 3400 K and luminosities from 1500 $L_\odot$ to 7000 $L_\odot$. All models include molecular opacities for the composition $(Y, Z) = (0.28, 0.02)$ and a horizontal averaging of opacity in convective regions. In some models turbulent pressure was also included.

From the results of this study, period-mass-radius relations have been derived for both fundamental mode and first overtone pulsation. The *PMR* relations have been compared to observations to see if the mode of pulsation can be identified.

Subject headings: stars: long-period variables — stars: pulsation

I. INTRODUCTION

In recent years a substantial volume of literature has been produced dealing with the physical characteristics of Mira variable stars. Despite this, considerable uncertainty still exists in estimating the radii and the effective temperatures of these objects. Measured values of Mira radii are strongly dependent on the wavelength bands used and on assumed distance scales. Angular diameters have been measured using occultations and speckle interferometry and may be as much as a factor of 2 larger if observations are made over broad visual wavelength bands rather than over narrow visual wavelength bands or in the infrared (Ridgway, Wells, and Joyce 1977; Labeyrie *et al.* 1977: Tsuji 1978; Bonneau *et al.* 1982). Labeyrie *et al.* (1977) found that the measured angular diameter depends strongly on wavelength due to the effects of TiO absorption features. They have argued that the optically thick regions of the atmosphere, when measured in the TiO bands, may extend several stellar radii above the continuum-forming layer.

The appropriate temperature scale for Miras is also uncertain. Fits of blackbody curves to infrared energy distributions using *JHKL* photometry (Robertson and Feast 1981) tend to give the lowest values. However, detailed fitting of the energy distributions for several Miras over the wavelength range from 1 to 5 mm yields higher temperatures than those found from blackbody fits (Scargle and Strecker 1979). The same is true for $R-I$ colors (Eggen 1975) calibrated using diameters for nonvariable red giants (Ridgway *et al.* 1980).

Because of uncertainties in the appropriate radii and effective temperatures for Miras, the mode of pulsation of these objects is being debated (e.g., Willson 1982*a*). If the cooler blackbody temperature scale of Robertson and Feast (1981) is assumed, pulsation is likely to be in the first overtone (e.g., Wood 1974; Fox and Wood 1982), while the Ridgway *et al.* (1980) temperature scale for nonvariable red giants would seem to indicate that fundamental mode pulsation is more likely (Willson 1982*a*).

In light of the uncertainties discussed above, it is the aim of this paper to investigate the possible modes of pulsation and their associated growth rates in the limit of infinitesimal oscillations over a wide range of effective temperatures and luminosities. In this way it is hoped that the actual asymptotic giant branch (AGB) of the H-R diagram, on which the Miras are believed to reside (e.g., Wood 1974), will be bracketed. In a similar approach, Fox and Wood (1982) recently investigated the linear pulsation characteristics of the more general class of long-period variables (LPVs) using selected AGBs.

In § II of this paper we present details of the physical assumptions made in this analysis, with particular attention paid to the modifications made in the standard treatment of the mixing length theory of convection. In § III, pulsational characteristics of the models are presented, and the results are discussed in § IV, with conclusions given in § V.

II. PHYSICAL ASSUMPTIONS

The structure of Mira envelopes is complex, involving extensive convection zones and significant amounts of radiation pressure (e.g., Keeley 1970; Wood 1974) as well as shock waves that produce periodic ionization/dissociation events (e.g., Willson, Wallerstein, and Pilachowski 1982). Extensive mass loss is also well documented (e.g., Knapp 1985; Knapp and Chang 1985). In this section some modifications to the standard model building and linear, nonadiabatic (LNA) pulsation code are presented which attempt to address some of the complexities of Miras.

a) Composition

The composition used in all models is the Ross-Aller (1976) mixture with the fraction, by mass, of helium and metals being $(Y, Z) = (0.28, 0.02)$. The equation-of-state and opacity tables are from the Los Alamos opacity library with contributions of several molecular species having been specially added at low temperatures.

b) Atmospheric Structure

In an attempt to minimize the errors introduced by using the diffusion theory in optically thin zones, the surface pressure and the optical depth at the center of the outermost zone were adjusted to obtain the best possible agreement with the model atmospheres of Johnson, Bernat, and Krupp (1980, hereafter JBK). These models assume LTE, are in hydrostatic equilibrium, and have neglected curvature (i.e., are plane-parallel). The contibution of molecules such as VO to the opacity has also been neglected. Unfortunately, when applied to Miras each of these approximations is weak. However, in the construction of the initial hydrostatic model envelopes, only the plane-parallel approximation and molecular contributions are likely to introduce significant errors.

The surface pressure P_S was adjusted by changing the amount of inertial mass assumed to lie above the outermost zone. The optical depth of the outermost zone τ_{top} defines the temperature in that zone through the relation

$$T_{top}^4 = \tfrac{3}{4} T_e^4 (\tau_{top} + \tfrac{2}{3}) .$$

Given P_S and τ_{top}, the integration proceeds inward and is tested to be sure that $T = T_e$ (effective temperature) at $r = R_e$ (photospheric radius). Figure 1 shows the effects on the envelope structure of a 0.8 $M_\odot$ model with $L = 5000\ L_\odot$ and $T_e = 3275$ K caused by varying τ_{top} and $f_a \equiv M_{IR}/M_{IR+1}$ (where M_{IR} is the mass of the outermost zone and M_{IR+1} is the inertial mass above the outermost zone). An extrapolated model atmosphere based on JBK is included for comparison. The fundamental mode nonadiabatic periods P_0 and linear growth rates η_0 for the models of Figure 1 are given in Table 1. It is reassuring to note that although the outer structure of the envelopes change significantly for various choices of τ_{top} and f_a, the pulsation periods and growth rates are relatively insensitive to these choices. This is probably a result of the dominance of convection in determining the temperature structure throughout most of the volume of these stars. The quantities f_a and τ_{top} were both set to 0.01 for the remainder of this study. Fox and Wood (1982) found a similar insensitivity of the fundamental mode period to the location of the outermost boundary.

TABLE 1

THE EFFECTS OF f_a AND τ_{top} ON P_0 AND η_0

Model	f_a	τ_{top}	P_0 (days)	η_0
A.....	0.01	0.01	347	2.72
B.....	0.005	0.001	342	3.16
C.....	0.01	0.001	342	3.24
D.....	0.1	0.001	339	3.39

c) The Inner Boundary Condition

In the present study a range of models with differing effective temperatures, luminosities, and masses have been tested for pulsational stability. After the specification of a particular model (i.e., choice of T_e, L, M_*) a large (actually infinite) number of possible solutions still exist for the stellar structure equations when convective model envelopes are calculated using the mixing length theory. The selection of a particular solution results from the choice of a value for the mixing length–to–pressure scale height ratio l/H_P. The value of l/H_P used here for a given model was chosen so that the envelope inner boundary would be consistent with the core mass–

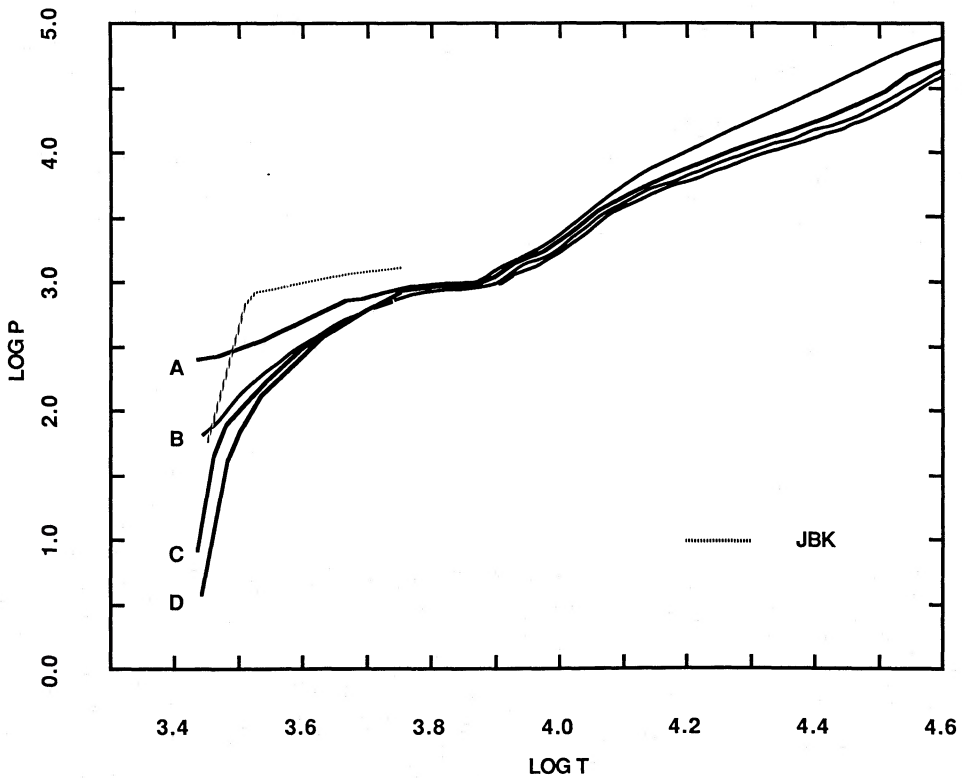

FIG. 1.—Effects of varying surface conditions on envelope structure. Models A, B, C, and D correspond to the models of Table 1. In all cases $M = 0.8\ M_\odot$, $L = 5000\ L_\odot$, $T = 3275$ K, and $l/H_P = 2.5$. An extrapolated plane-parallel model atmosphere of JBK has been included for comparison. The pressure is in dynes cm^{-2} and the temperature is in kelvins.

luminosity relation characteristic of AGB evolution. The $M_c - L$ relation adopted here is due to Iben and Truran (1978), with

$$L = 6.34 \times 10^4 (M_c - 0.44)(M_*/7)^{0.19} ,$$

where M_* is the total stellar mass, M_c is the mass of the degenerate carbon–oxygen core, and L is the total luminosity (with all variables in solar units). It should be noted that although M_c may be specified by the $M_c - L$ relation, $\sim 0.1\ M_\odot$ of material lies between the C–O core and the hydrogen-burning shell where the inward integrations were terminated. However, periods were found to be rather insensitive to small (<20%) errors in the estimated inner mass boundary. In this approach l/H_P is no longer a free parameter but is determined by the $M_c - L$ relation used.

d) Modifications to the Mixing-Length Theory

The mixing-length theory (Böhm-Vitense 1958) has been used here following the formalism presented in Cox and Giuli (1968). However, several changes have been made in an effort to remove some of the inconsistencies that exist in the standard treatment.

Using a slight modification of a scheme suggested by Deupree (1979), we have horizontally averaged the different opacities of rising and falling convective elements within each zone. The temperature difference between a hot, rising element or a cold, falling element and the ambient temperature is estimated by making use of the expression (Cox and Giuli 1968) for the change in temperature over one mixing length given by

$$\Delta T(l) = l \Delta \nabla T ,$$

where

$$\Delta \nabla T = \left(\frac{2}{\pi^2} \frac{H_c^2 T}{r^4 g \rho^2 c_p^2 l^4 Q} \right)^{1/2} ,$$

H_c is the convective flux,

$$Q \equiv - \left. \frac{\log \rho}{\log T} \right|_P ,$$

g is the local acceleration of gravity, C_p is the specific heat capacity, and all other quantities have their usual meanings. Assuming that the horizontal changes in density and pressure have a second-order effect on the opacity and are therefore negligible, the average opacity of a zone in a convective region is determined by

$$\frac{1}{\kappa_{\rm av}} = \frac{a}{\kappa(T_0 + T)} + \frac{b}{\kappa(T_0)} + \frac{c}{\kappa(T_0 - T)} ,$$

where a, b, and c are weighting factors ($a + b + c = 1$) and T_0 is the average temperature of the zone. Since H_c itself depends on $\kappa_{\rm av}$, several iterations are needed to determine ΔT for each zone. Without any specific constraints on the weighting factors a, b and c beyond normalization, we have arbitrarily set each constant equal to $\frac{1}{3}$.

The largest effect of the opacity averaging scheme was found to occur in the hydrogen ionization zone, where $\Delta T/T$ was as large as 0.4. It is also in ionization zones where the opacity is most temperature-dependent. Figure 2 shows both L_r/L_T, the ratio of the radiative luminosity to the total luminosity, and $\Delta T/T$ for the $0.8\ M_\odot$ model of Figure 1. Apparent is the rapid increase in convective luminosity for temperatures greater than 9000 K when the opacity averaging scheme is used. Without opacity averaging it is found that the onset of convection occurs nearer 7000 K. Since hydrogen ionization dominates the pulsational driving of Mira variables, it might be expected that opacity averaging would affect modal stability. It is worth noting, however, that although opacity averaging changes the static structure of these models significantly and increases fun-

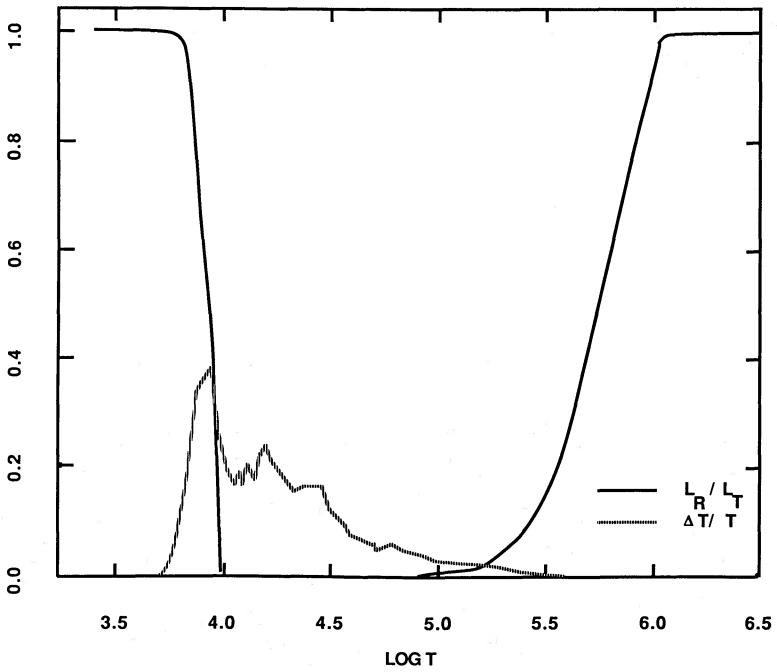

FIG. 2.—Radiative luminosity (L_r/L_t) and the convective element temperature difference ($\Delta T/T$) as a function of temperature. The maximum in $\Delta T/T$ corresponds to the top of the hydrogen ionization region where the opacity is highly temperature-dependent.

damental mode growth rates by as much as 30%, linear pulsation periods vary by less than 10%.

The effects of modifying the standard mixing length theory through the inclusion of a turbulent pressure term in the expression for the temperature gradient was also investigated in selected models. The turbulent pressure term results from convective motions and has the form

$$P_{\rm turb} = 1/2\rho V_c^2 ,$$

where V_c is the convective velocity. Because the temperature gradient directly influences the convective velocity, an iteration scheme was required to achieve a consistent solution. Results of the inclusion of the turbulent pressure term will be presented in § IV.

A major flaw exists in the standard mixing length theory when it is used to describe convective energy transport in pulsating stars: its lack of any time dependence. In the case of Mira variables, a typical time scale for convection, defined as the amount of time needed for a convective element to travel one mixing length, is $t_{\rm conv} \approx 0.3P_0$, where P_0 is the fundamental mode pulsation period of the star. For overtone pulsation $t_{\rm conv}/P$ will be even higher. Because of the approximately equal time scales for pulsation and convection, some sort of time-dependent formalism is needed. In LNA, convection is assumed to be "frozen in" and is not allowed to adapt at all to a changing environment. In view of the similarity between convection and pulsation time scales, such an assumption may not be valid. However, Langer's (1971) finding in the linear regime that pulsation periods and growth rates are fairly insensitive to whether convection was "frozen in" or allowed to adjust instantaneously gives some hope that perhaps our results are not completely unrealistic.

III. LINEAR PULSATION CHARACTERISTICS

A range of stellar parameters has been investigated in light of uncertainties in the masses, the appropriate temperature scale, and the radii of Miras. About 100 models have been tested for fundamental-mode as well as for first- and second-overtone pulsation using the linear, nonadiabatic eigenvector method suggested by Castor (1971) and described in detail by Langer (1969). Models of 0.8, 1.0, 1.4, and 2.0 $M_\odot$ have been considered for temperatures ranging from 2700 K to 3400 K and luminosities from 1500 $L_\odot$ to 7000 $L_\odot$. In all cases, horizontal averaging of the opacity in convective zones has been included, but the turbulent pressure term has been added in only a small number of models.

a) Static Models

The static structure of AGB stars has been described in detail many times (e.g., Keeley 1970; Wood 1974; Ostlie 1982) and is not discussed again here. Structure changes caused by opacity averaging are described in § II. The addition of the turbulent pressure term was found to have little influence on the static AGB models beyond the slight increases required in l/H_P in order to satisfy the boundary conditions.

b) Adiabatic and Nonadiabatic Pulsation Periods

Results of the linear stability analysis for model enevelopes with turbulent pressure neglected are given in Table 2. Included are the adiabatic and nonadiabatic pulsation periods for the fundamental mode and the first and second overtones, as well as the pulsation constants $Q \equiv P(\rho/\rho_\odot)^{1/2}$, growth rates η, and the value of l/H_P required to satisfy both the surface and inner boundary conditions for each model.

For overtone pulsation the adiabatic and nonadiabatic periods differ little (<10% everywhere), with the adiabatic period always the smaller of the two. For fundamental mode pulsation the periods may be substantially different, with the adiabatic period being almost twice the nonadiabatic value for the lowest mass models having the largest radii. Clearly, nonadiabatic effects are most significant in fundamental-mode pulsation, becoming increasingly important as the masses of the models decrease and their radii increase.

c) The Work Function

As has been found by other investigators (e.g., Langer 1969), the dominant driving mechanism for all models investigated results from hydrogen ionization. This can be seen immediately by plotting both $\Gamma_3 - 1$ and the work function per zone versus temperature;

$$\Gamma_3 - 1 \equiv \left.\frac{d \log T}{d \log \rho}\right|_{\rm ad} ,$$

where ad refers to adiabatic compression or expansion. If an adiabatic compression is carried out for a gas not undergoing ionization or dissociation, the energy of compression will result in a higher average kinetic energy for each particle and a correspondingly higher temperature. Because of the increase in temperature with increasing density, $\Gamma_3 - 1$ will remain nearly constant over most of the stellar interior. If, on the other hand, adiabatic compression takes place in a region of partial ionization, the compressional energy will go into ionization rather than kinetic energy, and the temperature will remain more nearly constant with increasing density, resulting in a drop in $\Gamma_3 - 1$.

For a 1.0 $M_\odot$ model with $L = 5000\ L_\odot$, $T_e = 3000$ K, and $l/H_P = 2.6$, $\Gamma_3 - 1$ and the fundamental mode work function have been plotted as a function of log T in Figure 3. Note the dominance of the positive work function in the hydrogen ionization zone near 10,000 K. Although damping is present in other zones, the negative contribution to the work function is several orders of magnitude smaller than the driving that is present in the hydrogen ionization region. This is evident in the very large linear growth rates common to fundamental-mode pulsation in these models. For the model represented in Figure 3, $\eta_0 = 2.5$; the pulsation amplitude e-folds in just $0.4P_0$!

For each of the cases studied here, only second-overtone oscillations were ever found to be pulsationally stable (i.e., <0), and then only for a small number of models.

d) Growth Rates and Nonadiabacity

It is the presence of nonadiabatic effects that governs the growth or decay of stellar pulsations, and the degree to which oscillations are nonadiabatic has been found to be well correlated with the linear growth rates of the fundamental mode. Inspection of Table 2 shows that η_0 tends to be larger for models of lower mass and larger radius. Qualitatively, this results because heat exchange is more rapid in a low-density star.

The amount of nonadiabacity in stellar pulsations may be estimated by comparing the thermal (or Kelvin) time scale to the pulsation period. If the Kelvin time is of the same order as the pulsation period, adiabacity becomes a poor assumption. The Kelvin time (Cox 1980) may be estimated by considering

TABLE 2

PERIODS, Q-VALUES, AND GROWTH RATES FOR LINEAR MODELS WITHOUT TURBULENT PRESSURE

L ($L_\odot$)	T_e (K)	l/H_P	P_0(ad)[a] (days)	P_0 (days)	Q_0 (days)	η_0	P_1(ad)[a] (days)	P_1 (days)	Q_1 (days)	η_1	P_2(ad)[a] (days)	P_2 (days)	Q_2 (days)	η_2
						$M = 0.8\ M_\odot$								
1500.....	2800	1.61	197.2	197.0	0.0834	0.851	90.8	93.1	0.0394	0.336	57.2	59.6	0.0251	0.094
	3000	1.81	148.4	147.9	0.0770	0.704	73.9	75.2	0.0392	0.373	47.1	48.6	0.0253	0.161
	3200	2.00	115.2	114.6	0.0724	0.589	60.6	61.3	0.0388	0.396	39.1	40.0	0.0253	0.216
	3400	2.22	90.8	90.2	0.0684	0.514	50.2	50.6	0.0384	0.418	32.7	33.3	0.0253	0.263
2000.....	2700	1.66	312.5	307.5	0.0941	1.615	125.5	130.3	0.0399	0.407	78.2	82.5	0.0253	0.030
	2800	1.76	267.7	263.4	0.0899	1.437	112.9	116.6	0.0398	0.486	70.4	73.9	0.0253	0.083
	3000	1.93	200.1	196.5	0.0825	1·178	92.1	94.1	0.0395	0.519	57.9	60.1	0.0253	0.184
	3200	2.25	152.9	150.3	0.0765	1.013	75.9	77.0	0.0394	0.545	48.2	49.6	0.0253	0.241
	3400	2.38	122.3	120.0	0.0733	0.914	62.7	63.4	0.0387	0.580	40.0	40.9	0.0250	0.297
3000.....	2700	1.91	497.5	448.9	0.1013	3.142	169.3	178.2	0.0402	0.589	104.9	111.9	0.0253	−0.023
	2800	2.05	422.3	386.5	0.0973	2.842	153.1	160.2	0.0403	0.644	94.1	99.9	0.0252	0.018
	3000	2.27	310.5	287.9	0.0892	2.309	125.1	129.2	0.0400	0.770	77.3	81.1	0.0251	0.145
	3200	2.57	233.2	219.1	0.0823	1.939	103.3	105.8	0.0397	0.832	64.4	66.9	0.0251	0.239
	3400	2.75	184.0	173.5	0.0782	1.714	85.6	87.0	0.0392	0.892	53.6	55.3	0.0249	0.324
5000.....	2700	2.20	1017.0	667.5	0.1027	5.503	244.9	265.4	0.0408	0.726	153.2	165.9	0.0255	−0.105
	2800	2.31	821.6	580.0	0.0995	4.993	221.4	238.1	0.0409	0.857	136.1	147.3	0.0253	−0.110
	3000	2.66	568.6	434.2	0.0917	4.283	182.3	192.4	0.0406	1.109	110.3	117.0	0.0247	−0.045
	3200	2.91	420.2	338.9	0.0868	3.690	151.7	157.9	0.0405	1.274	91.8	96.3	0.0247	0.109
	3400	3.13	322.8	270.5	0.0831	3.197	127.0	130.6	0.0401	1.371	77.5	80.4	0.0247	0.258
7000.....	3000	2.55	1053.1	546.2	0.0896	6.948	227.8	239.7	0.0390	1.299	136.4	146.6	0.0240	−0.235
	3200	2.92	714.9	439.2	0.0874	6.042	191.4	200.8	0.0400	1.439	112.7	117.8	0.0234	−0.143
	3400	3.30	508.3	348.1	0.0831	5.096	161.5	168.6	0.0402	1.578	95.3	98.2	0.0234	0.021
						M = 1.0 $M_\odot$								
1500.....	2700	1.40	184.4	185.3	0.0787	0.436	91.7	93.6	0.0397	0.220	58.4	60.4	0.0256	0.066
	2800	1.50	158.8	159.4	0.0755	0.389	82.1	83.5	0.0395	0.233	52.7	54.3	0.0257	0.096
	3000	1.71	121.0	121.2	0.0706	0.339	66.4	67.2	0.0392	0.259	43.1	44.0	0.0256	0.141
	3200	1.87	94.6	94.6	0.0669	0.270	54.1	54.5	0.0386	0.268	35.5	36.2	0.0256	0.186
	3400	2.07	75.0	74.9	0.0635	0.229	44.9	45.2	0.0383	0.273	29.8	30.2	0.0254	0.208
2000.....	2700	1.53	248.0	248.3	0.0850	0.767	113.4	116.4	0.0398	0.307	71.4	74.4	0.0255	0.074
	2800	1.68	210.7	210.8	0.0805	0.688	102.5	104.8	0.0400	0.325	65.0	67.4	0.0257	0.108
	3000	1.90	159.1	158.8	0.0746	0.558	83.1	84.4	0.0396	0.356	53.5	55.0	0.0258	0.170
	3200	2.09	124.0	123.6	0.0704	0.467	68.1	68.7	0.0392	0.380	44.4	45.3	0.0258	0.232
	3400	2.22	97.7	97.3	0.0665	0.387	56.6	57.0	0.0389	0.385	37.2	37.8	0.0258	0.264
3000.....	2700	1.79	381.6	372.2	0.0940	1.736	153.6	159.3	0.0402	0.470	95.2	100.5	0.0254	0.048
	2800	1.91	322.2	315.7	0.0889	1.423	139.6	143.7	0.0405	0.510	87.3	91.4	0.0257	0.113
	3000	2.21	239.5	234.4	0.0812	1.176	113.9	116.2	0.0402	0.580	71.9	74.6	0.0258	0.215
	3200	2.47	183.4	179.7	0.0755	1.004	93.7	95.1	0.0400	0.609	59.8	61.5	0.0258	0.281
	3400	2.61	144.7	142.0	0.0716	0.855	77.3	78.0	0.0393	0.619	49.8	50.9	0.0257	0.333
5000.....	2800	2.27	572.1	502.8	0.0965	3.042	206.3	216.2	0.0415	0.843	126.8	135.1	0.0259	0.034
	3000	2.61	414.4	373.8	0.0883	2.546	167.7	173.5	0.0410	0.956	103.4	108.6	0.0256	0.155
	3200	2.93	311.5	285.7	0.0819	2.154	138.4	141.8	0.0406	1.031	86.3	89.7	0.0257	0.265
	3400	3.21	241.8	224.3	0.0771	1.863	115.1	117.0	0.0402	1.072	72.4	74.8	0.0257	0.359
7000.....	3000	2.97	613.3	487.1	0.0894	3.843	215.3	226.7	0.0416	1.173	131.0	139.0	0.0255	−0.006
	3200	3.24	453.7	377.0	0.0839	3.235	179.2	185.9	0.0414	1.367	109.4	114.4	0.0255	0.162
	3400	3.50	348.8	298.1	0.0796	2.806	148.8	152.5	0.0407	1.412	91.8	95.1	0.0254	0.280
						$M = 1.4\ M_\odot$								
1500.....	2700	1.22	140.9	141.4	0.0710	0.134	78.2	79.1	0.0397	0.124	50.4	51.5	0.0259	0.055
	2800	1.24	122.5	122.8	0.0688	0.116	69.9	70.6	0.0396	0.129	45.3	46.2	0.0259	0.072
	3000	1.42	94.1	94.2	0.0649	0.096	56.0	56.4	0.0389	0.140	36.8	37.4	0.0258	0.104
	3200	1.65	74.0	74.0	0.0619	0.080	45.6	45.8	0.0383	0.145	30.3	30.7	0.0257	0.121
	3400	1.85	59.3	59.3	0.0595	0.062	37.4	37.5	0.0376	0.148	25.3	25.5	0.0256	0.137
2000.....	2700	1.36	185.2	185.9	0.0753	0.252	97.4	98.8	0.0400	0.182	62.1	63.8	0.0258	0.074
	2800	1.45	159.9	160.3	0.0724	0.226	87.8	88.9	0.0401	0.191	56.3	57.6	0.0260	0.095
	3000	1.57	122.3	122.4	0.0680	0.174	70.6	71.3	0.0396	0.205	46.0	46.8	0.0260	0.142
	3200	1.84	95.7	95.7	0.0645	0.149	57.5	57.9	0.0390	0.213	37.9	38.4	0.0259	0.162
	3400	2.02	76.6	76.5	0.0619	0.117	47.2	47.4	0.0383	0.213	31.5	31.8	0.0257	0.189
3000.....	2700	1.53	275.8	276.1	0.0825	0.552	133.7	136.4	0.0407	0.303	84.2	87.2	0.0260	0.112
	2800	1.69	236.8	236.8	0.0789	0.500	120.2	122.3	0.0407	0.319	76.2	78.6	0.0262	0.140
	3000	1.84	179.6	179.1	0.0734	0.389	97.5	98.5	0.0404	0.347	62.6	64.1	0.0263	0.212
	3200	2.10	139.3	138.8	0.0690	0.338	79.4	79.9	0.0397	0.365	51.5	52.4	0.0261	0.258
	3400	2.24	110.4	110.1	0.0657	0.266	65.7	65.9	0.0393	0.357	43.1	43.6	0.0260	0.274
5000.....	2700	1.93	470.2	457.7	0.0932	1.487	198.5	204.2	0.0416	0.551	123.0	129.1	0.0263	0.129
	2800	1.97	400.3	390.0	0.0886	1.286	178.5	182.6	0.0415	0.597	111.0	115.9	0.0263	0.196
	3000	2.31	297.3	290.7	0.0812	1.046	145.2	147.4	0.0412	0.634	91.4	94.4	0.0264	0.279
	3200	2.46	227.8	223.4	0.0757	0.850	118.9	120.1	0.0407	0.653	75.6	77.6	0.0263	0.342
	3400	2.71	178.4	175.4	0.0713	0.694	98.5	98.9	0.0402	0.663	63.4	64.7	0.0263	0.400

TABLE 2—*Continued*

L ($L_\odot$)	T_e (K)	l/H_P	P_0(ad)[a] (days)	P_0 (days)	Q_0 (days)	η_0	P_1(ad)[a] (days)	P_1 (days)	Q_1 (days)	η_1	P_2(ad)[a] (days)	P_2 (days)	Q_2 (days)	η_2
$M = 1.4\ M_\odot$—*Continued*														
7000.....	2800	2.36	576.6	533.0	0.0940	2.232	231.0	283.5	0.0421	0.829	142.1	150.1	0.0265	0.150
	3000	2.65	422.4	396.0	0.0860	1.842	188.1	192.1	0.0417	0.905	116.8	121.7	0.0264	0.271
	3200	2.92	318.8	302.7	0.0797	1.476	153.9	156.1	0.0411	0.954	96.8	100.1	0.0264	0.361
	3400	3.13	248.8	237.8	0.0751	1.241	128.2	129.1	0.0408	0.969	81.3	83.6	0.0263	0.454
$M = 2.0\ M_\odot$														
1500.....	2700	1.00	112.7	112.8	0.0677	0.036	64.5	64.9	0.0390	0.065	42.1	42.7	0.0256	0.037
	2800	1.09	98.1	98.2	0.0657	0.033	57.2	57.5	0.0385	0.066	37.7	38.2	0.0256	0.043
	3000	1.22	76.6	76.6	0.0631	0.023	45.6	45.8	0.0378	0.066	30.8	31.1	0.0256	0.058
	3200	1.42	60.5	60.5	0.0605	0.019	36.8	39.9	0.0369	0.069	25.4	25.6	0.0255	0.068
	3400	1.60	48.9	48.9	0.0586	0.016	29.9	30.0	0.0359	0.073	21.0	21.1	0.0254	0.083
2000.....	2700	1.11	146.5	146.7	0.0710	0.068	81.2	81.9	0.0396	0.096	52.3	53.1	0.0257	0.055
	2800	1.22	125.9	126.0	0.0680	0.063	72.2	72.7	0.0392	0.107	46.9	47.6	0.0257	0.065
	3000	1.38	96.8	96.9	0.0643	0.053	57.2	57.6	0.0382	0.109	37.9	38.3	0.0254	0.085
	3200	1.52	76.9	76.9	0.0620	0.039	46.2	46.3	0.0373	0.102	31.1	31.4	0.0253	0.095
	3400	1.69	62.4	62.4	0.0603	0.027	38.1	38.2	0.0369	0.097	26.2	26.4	0.0255	0.100
3000.....	2700	1.27	215.1	215.5	0.0770	0.157	113.9	115.2	0.0411	0.170	72.1	73.7	0.0263	0.095
	2800	1.41	184.9	185.1	0.0737	0.142	101.0	102.0	0.0406	0.177	64.5	65.7	0.0262	0.111
	3000	1.60	140.4	140.5	0.0688	0.117	80.7	81.3	0.0398	0.186	52.3	53.1	0.0260	0.139
	3200	1.81	109.7	109.7	0.0652	0.095	65.2	65.6	0.0390	0.190	43.0	43.5	0.0258	0.158
	3400	1.98	87.6	87.6	0.0624	0.077	52.9	53.1	0.0379	0.187	35.4	35.7	0.0255	0.172
5000.....	2700	1.61	349.5	349.0	0.0850	0.502	169.0	171.7	0.0418	0.332	105.1	108.4	0.0264	0.150
	2800	1.71	301.4	300.8	0.0817	0.417	151.1	153.2	0.0416	0.341	94.9	97.5	0.0265	0.184
	3000	1.95	226.0	225.5	0.0753	0.345	121.6	122.8	0.0410	0.362	77.1	78.8	0.0263	0.226
	3200	2.17	175.6	175.0	0.0709	0.264	99.0	99.5	0.0403	0.366	63.7	64.7	0.0262	0.273
	3400	2.29	139.5	139.1	0.0676	0.209	81.2	81.4	0.0395	0.362	53.0	53.6	0.0260	0.300
7000.....	2700	1.85	491.3	485.0	0.0917	0.999	218.4	223.2	0.0423	0.488	134.7	140.2	0.0265	0.167
	2800	1.98	420.5	415.3	0.0876	0.853	197.4	200.8	0.0423	0.517	122.4	126.6	0.0267	0.222
	3000	2.22	312.5	308.5	0.0800	0.689	159.0	160.5	0.0417	0.559	99.5	102.1	0.0265	0.305
	3200	2.46	240.4	237.8	0.0749	0.537	129.7	130.4	0.0411	0.563	82.2	83.9	0.0264	0.354
	3400	2.68	189.5	187.8	0.0709	0.420	106.3	106.6	0.0402	0.553	68.5	69.6	0.0263	0.396

[a] Adiabatic period.

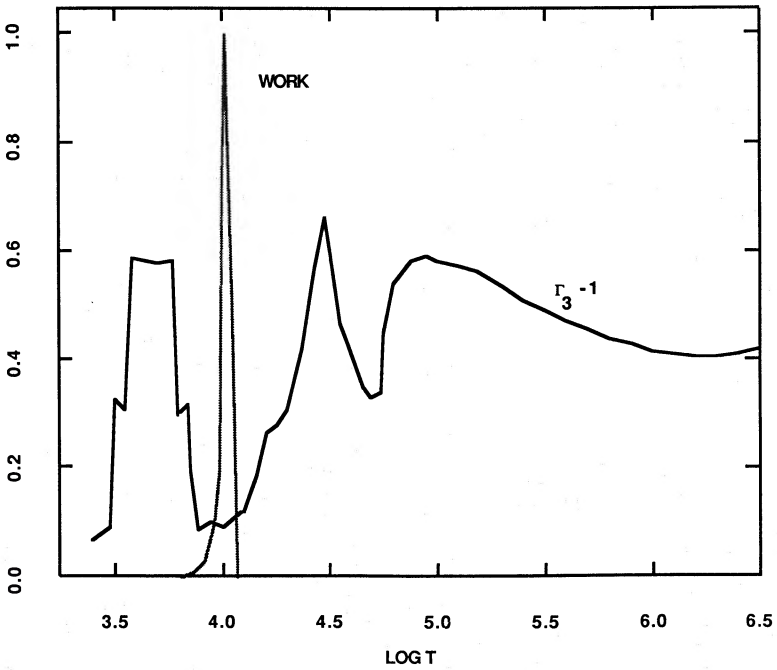

FIG. 3.—Locations of ionization and fundamental-mode pulsational driving regions. The second helium ionization, first helium-hydrogen ionization, and molecular dissociation regions are evident by the minima in $\Gamma_3 - 1$ at log $T = 4.7$, 4.0, and 3.4 respectively. The work function is in arbitrary units.

the ratio of the total internal (thermal) energy content of a star to its luminosity:

$$t_K \approx E_{th}/L .$$

The amount of thermal energy may be related to the star's gravitational energy through the use of the virial theorem, yielding the expression

$$t_K \approx 2 \times 10^7 \frac{M^2}{LR} \text{ yr} ,$$

where M, L, and R, are all in solar units. Finally, using the expression for the pulsation period in terms of the pulsation constant Q, the ratio of the Kelvin time to the period of oscillation of a star may be written as

$$\frac{t_K}{P_i} \approx 7 \times 10^9 \frac{M^{5/2}}{R^{5/2} L Q_i} ,$$

where Q_i is in days. Since Q_i is only slowly varying for a given mode, it is apparent that the degree of nonadiabacity is a strong function of both the mass and the radius, as expected.

For a Mira with $M = 2.0\ M_\odot$, $L = 2000\ L_\odot$, $R = 200\ R_\odot$, and $Q_0 = 0.07$ day we have $t_K = 200$ yr, much longer than any observed period ($t_K/p_0 = 500$). However, for a Mira with $M = 0.8\ M_\odot$, $L = 7000\ L_\odot$, $R = 300\ R_\odot$, and $Q_0 = 0.089$ days, the Kelvin time is $t_K = 6$ yr, compared with a fundamental mode period of ~ 1.5 yr ($t_K/p_0 = 4.1$). Clearly, in the latter case nonadiabatic effects will be pronounced. When overtone pulsation is considered, nonadiabatic effects will certainly be less severe because of the much shorter periods.

Figure 4 demonstrates the dependence of fundamental-mode growth rates on the degree of nonadiabacity. For models having a Kelvin time much larger than the pulsation period, oscillations are nearly adiabatic and the resulting growth rates are small. If the Kelvin time is near the fundamental-mode period, growth rates may be quite large.

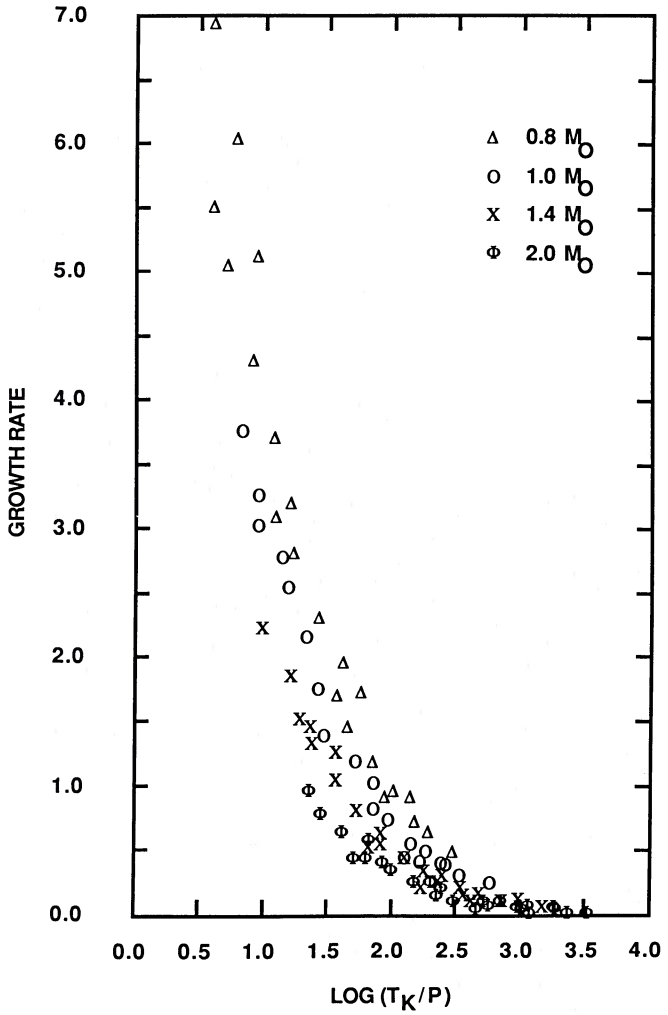

FIG. 4.—Effect of nonadiabaticity on fundamental mode growth rates for models with turbulent pressure neglected. The growth rate is seen to be a strong function of the Kelvin time–to–pulsation period ratio t_K/P.

e) The Effects of Turbulent Pressure

The inclusion of the turbulent pressure term in pulsation models apparently leads to more severe nonadiabacity, as is evident from the periods and growth rates given in Table 3. Models 1 and 2 differ only in the use of the turbulent pressure term, with the result that periods and growth rates have changed appreciably. The adiabatic fundamental mode period increased by more than a factor of 2 when turbulent pressure was included, while the nonadiabatic period increased by $\sim 25\%$. The growth rate for fundamental-mode pulsation also increased significantly (69%).

The other models of Table 3 may be compared directly with their counterparts in Table 2. As expected from the analysis of the last section, the amount by which the adiabatic and nonadiabatic fundamental-mode periods differ, as well as the magnitude of the linear, fundamental-mode growth rates, depend strongly on the mass, radius, and luminosity of the models, with the less massive models of larger radius and greater luminosity being least adiabatic. Presumably, the enhanced nonadiabacity of the turbulent pressure models is due to less material supporting the overlying layers, with the result that the lower density allows for more rapid thermal adjustment

TABLE 3

EFFECT OF TURBULENT PRESSURE

Model	M ($M_\odot$)	L ($L_\odot$)	T_e (K)	l/H_P	P_0(ad)[a] (days)	P_0 (days)	Q_0 (days)	η_0	P_1(ad)[a] (days)	P_1 (days)	Q_1 (days)	η_2	P_2(ad) (days)	P_2 (days)	Q_2 (days)	η_2	P_{turb}
1.....	0.8	5000	3275	2.66	394.0	339.8	0.0933	3.823	142.3	148.9	0.0409	0.610	83.9	91.0	0.0250	−0.132	No
2.....	0.8	5000	3275	2.88	898.8	422.9	0.1161	6.454	159.0	164.9	0.0453	0.662	89.1	95.8	0.0263	−0.163	Yes
3.....	0.8	5000	3000	2.53	2616.6	591.1	0.1248	7.400	203.0	214.1	0.0452	0.530	115.5	132.0	0.0279	−0.231	Yes
4.....	1.4	5000	3000	2.00	332.6	328.6	0.0918	1.322	150.9	154.9	0.0433	0.401	93.6	97.7	0.0273	+0.078	Yes
5.....	1.4	3000	3000	1.52	193.7	194.3	0.0796	0.388	100.4	101.9	0.0418	0.218	63.2	64.8	0.0265	+0.090	Yes
6.....	1.4	3000	2700	1.30	298.6	301.2	0.0900	0.534	137.6	141.2	0.0422	0.194	85.4	89.4	0.0267	+0.035	Yes

[a] Adiabatic period.

between adjacent zones. This simple picture is complicated somewhat, however, by the higher values of l/H_P needed in the turbulent pressure models in order to increase the density sufficiently to meet the surface and inner boundary conditions. With the larger values of l/H_P, a convective element is able to traverse an increased number of pressure scale heights, allowing thermal information to be transported further, again enhancing nonadiabatic effects.

IV. DISCUSSION

a) The PMR Relations

Results of the linear, nonadiabatic pulsation analysis may be compared with observations through period-mass-radius (*PMR*) relations, of which the expression for the pulsation constant is an example. To find the dependence of period (or equivalently, Q) on mass and radius, a least-squares fit of the results given in Table 2 (models without turbulent pressure) was used. For fundamental-mode pulsation,

$$\log P_0 = -1.92 - 0.73 \log M + 1.86 \log R ,$$

and for first-overtone pulsation,

$$\log P_1 = -1.60 - 0.51 \log M + 1.59 \log R ,$$

where periods are given in days and the mass and radius are in solar units. The *PMR* relations provide a means for rapid interpolation between models calculated here and may also be used (with caution) to extrapolate to masses and radii not considered in this study.

Fox and Wood (1982) have also derived a *PMR* relation for fundamental-mode pulsation from their survey of LPVs along a selected AGB. For stars with $0.8 \leq M/M_\odot \leq 3.0$ and the composition $(Y, Z) = (0.30, 0.02)$, they find $P_0 = Q_0{}^1 M^{-0.8} R^2$, where $Q_0{}^1 = 6.1 \times 10^{-3}$ days. In light of the different assumptions made in the two studies, this is in good agreement with the relation derived here, the largest discrepancies (18%) occurring for low-mass models of large radius. The *PMR* relations found here also give periods agreeing with some of the lowest luminosity (1800 $L_\odot$) nonlinear models of Tuchman, Sack, and Barkat (1979) but deviate significantly when applied to models having large luminosities and radii ($L = 10{,}000\ L_\odot$, $R = 7500\ R_\odot$). Extrapolations of this magnitude are probably not justified, however.

b) Comparison with Observations

In Figure 5 lines of constant mass have been plotted in the (log P, log R)-plane for both fundamental-mode (*solid lines*) and first-overtone (*broken lines*) pulsation using the *PMR* relations derived above. Also included in the diagram are observational data points for five stars based on occultation and speckle interferometry data obtained by a number of researchers and compiled by Willson (1982*b*). When several radius estimates were given for a particular star, the smallest value was generally selected with the hope that it more nearly represents the photosphere of the object rather than a sampling of the extended atmosphere or circumstellar shell. Two values are given for the radius of each star, based on whether the stellar disk is assumed to be of uniform brightness or is limb-darkened. It should be remembered that the values obtained for the radii of Miras depend strongly on the wavelength bands used to measure the angular diameters as well as on the assumed distance scale, here based on the *K*-

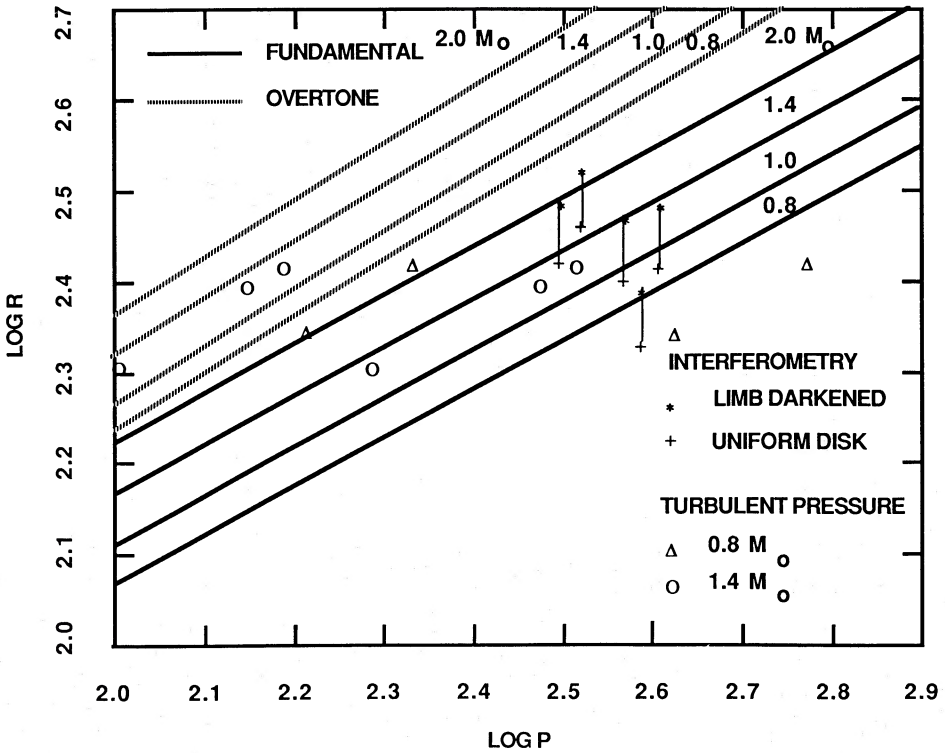

FIG. 5.—*PMR* relations for fundamental-mode and first-overtone pulsation with turbulent pressure neglected (solid and broken lines respectively). Fundamental-mode and first-overtone periods for five models with turbulent pressure have also been included. Interferometry data from five stars (Willson 1982*b*) have been included for comparison; R Leo (313 d), *o* Cet (332 d), U Ori (372 d), S Vir (388 d), and χ Cyg (407 d). The radius is in solar units and the period is in days.

magnitudes of Robertson and Feast (1981). Thus, the radii displayed in Figure 5 are subject to significant uncertainty.

For the radii assumed here, apparently fundamental-mode pulsation (with turbulent pressure neglected) is more consistent with observed periods than is first-overtone pulsation. Furthermore, it does not appear likely that decreasing the mass of models will be sufficient to allow for overtone pulsation. With a lower limit of $\sim 0.6\ M_\odot$, a consequence of the $M_c - L$ relation for AGB stars, overtone periods may be only slightly larger than those found for the $0.8\ M_\odot$ models and certainly not of the magnitude required here.

Using the Ridgway *et al.* (1980) temperature scale, Wood (1981) finds that fundamental-mode pulsation is most likely for the six shortest period objects listed in Table 1 of his paper, stars with $T_e > 3300$ K and $R < 300\ R_\odot$, while first-overtone pulsation is indicated for the three remaining longer period objects having $T_e < 3200$ K and $R > 400\ R_\odot$. Using the *PMR* relations determined here, we reach the same conclusions for the data given in his paper. Clearly, accurate determinations of radii are required to settle the question of the mode of pulsation.

c) *Turbulent Pressure*

The inclusion of turbulent pressure has been explored only sparingly in this linear survey because of the time-consuming nature of the iteration scheme required, but some conclusions concerning its effects may be drawn. The five turbulent-pressure models of Table 3 have been included in Figure 5 with only small changes in the first-overtone periods indicated. However, for fundamental-mode pulsation, periods have increased significantly, particularly for the lowest mass models (36%). Apparently turbulent pressure is an important effect and only enhances the difference between modes, allowing a wider range of radii at a given fundamental-mode period for the masses considered.

V. CONCLUSIONS

Although this linear survey of the Mira instability region of the H-R diagram seems to be consistent with fundamental-mode pulsation, significant uncertainties still exist in both theory and in the interpretation of observations. Theoretical uncertainties arise primarily in the treatment of convective energy transport. Questions concerning opacity averaging in convective regions, the use of turbulent pressure, and time-dependent convection all need to be addressed carefully when studying Mira variable stars. Observationally, identification of the true location of the AGB is necessary before linear results can be expected to answer the question of the mode of oscillation.

The authors wish to thank Dr. L A. Willson and Dr. J. H. Cahn for their valuable comments.

REFERENCES

Böhm-Vitense, E. 1958, *Zs. Ap.*, **46**, 108.
Bonneau, D., Foy, R., Blazit, A., and Labeyrie, A., 1982, *Astr. Ap.*, **106**, 235.
Castor, J. I. 1971, *Ap. J.*, **166**, 109.
Cox, J. P. 1980, *Theory of Stellar Pulsation* (Princeton: Princeton University Press).
Cox, J. P., and Giuli, R. T. 1968, *Principles of Stellar Structure* (New York: Gordon and Breach).
Deupree, R. G. 1979, *Ap. J.*, **234**, 228.
Eggen, O. 1975, *Ap. J.*, **195**, 661.
Fox, M. W., and Wood, P. R. 1982, *Ap. J.*, **259**, 198.
Iben, I. Jr., and Truran, J. W. 1978, *Ap. J.*, **220**, 980.
Johnson, H. R., Bernat, A. P., and Krupp, B. M. 1980, *Ap. J. Suppl.*, **42**, 501 (JBK).
Keeley, D. A. 1970, *Ap. J.*, **161**, 643.
Knapp, G. R. 1985, *Ap. J.*, **293**, 273.
Knapp, G. R., and Chang, K. M. 1985, *Ap. J.*, **293**, 281.
Labeyrie, A., Koechliu, L., Bonneau, D., Blazit, A., and Foy, R. 1977, *Ap. J. (Letters)*, **218**, L75.
Langer, G. E. 1969, Ph.D. thesis, University of Colorado.
Langer, G. E. 1971, *M.N.R.A.S.*, **155**, 199.
Ostlie, D. A. 1982, Ph.D. thesis, Iowa State University.
Ridgway, S. T., Joyce, R. R., White, N. M., and Wing, R. F. 1980, *Ap. J.*, **236**, 126.
Ridgway, S. T., Wells, D. C., and Joyce, R. R. 1977, *A.J.*, **82**, 414.
Robertson, B. S. C., and Feast, M. W. 1981, *M.N.R.A.S.*, **196**, 111.
Ross, J. E., and Aller, L. H. 1976, *Science*, **191**, 1223.
Scargle, J. D., and Strecker, D. W. 1979, *Ap. J.*, **228**, 838.
Tsuji, T. 1978, *Pub. A.S.P.*, **30**, 435.
Tuchman, Y., Sack, N., and Barkat, Z. 1979, *Ap. J.*, **234**, 217.
Willson, L. A. 1982*a*, in *Pulsations in Classical and Cataclysmic Variable Stars*, ed. J. P. Cox and Carl J. Hansen (Boulder, CO: JILA), p. 269.
———. 1982*b*, *Bull. AAS*, **13**, 803.
Willson, L. A., Wallerstein, G., and Pilachowski, C. A. 1982, *M.N.R.A.S.*, **192**, 483.
Wood, P. R. 1974, *Ap. J.*, **190**, 609.
———. 1981, in *Physical Processes in Red Giants*, ed. I. Iben and A. Renzini (Dordrecht: Reidel), p. 205.

ARTHUR N. COX: Theoretical Division, MS B288, Los Alamos National Laboratory, P.O. Box, 1663, Los Alamos, NM 87545

DALE A. OSTLIE: Physics Department, MS 2508, Weber State College, Ogden, UT 84408